In Silico Pharmacology (2026) 14:40
https://doi.org/10.1007/s40203-025-00539-7

RESEARCH

In silico prediction, molecular docking and simulation of natural flavonoid apigenin and xanthoangelol E against human metapneumovirus

Hasan Huzayfa Rahaman[1] · Afsana Khan[2] · Nadim Sharif[1,3] · Wasifuddin Ahmed[1] · Nazmul Sharif[4] · Rista Majumder[5] · Silvia Aparicio Obregon[6,7,8] · Rubén Calderón Iglesias[6,8,9] · Isabel De la Torre Díez[10] · Shuvra Kanti Dey[1]

Received: 24 August 2025 / Accepted: 20 December 2025

Abstract

Human metapneumovirus (hMPV) is one of the potential pandemic pathogens, and it is a concern for elderly subjects and immunocompromised patients. There is no vaccine or specific antiviral available for hMPV. We conducted an in-silico study to predict initial antiviral candidates against human metapneumovirus. Our methodology included protein modeling, stability assessment, molecular docking, molecular simulation, analysis of non-covalent interactions, bioavailability, carcinogenicity, and pharmacokinetic profiling. We pinpointed four plant-derived bio-compounds as antiviral candidates. Among the compounds, apigenin showed the highest binding affinity, with values of − 8.0 kcal/mol for the hMPV-F protein and −7.6 kcal/mol for the hMPV-N protein. Molecular dynamic simulations and further analyses confirmed that the protein-ligand docked complexes exhibited acceptable stability compared to two standard antiviral drugs. Additionally, these four compounds yielded satisfactory outcomes in bioavailability, drug-likeness, and ADME-Tox (absorption, distribution, metabolism, excretion, and toxicity) and STopTox analyses. This study highlights the potential of apigenin and xanthoangelol E as an initial antiviral candidate, underscoring the necessity for wet-lab evaluation, preclinical and clinical trials against human metapneumovirus infection.

Keywords Human metapneumovirus · Antivirals · Drug discovery · In-silico · Molecular docking · Dynamic simulation · Pharmacokinetics · ADME-Tox

Hasan Huzayfa Rahaman and Afsana Khan have contributed equally.

✉ Nadim Sharif
nadim@juniv.edu

✉ Shuvra Kanti Dey
shuvradey@yahoo.com

[1] Department of Microbiology, Jahangirnagar University, Savar 1342, Dhaka, Bangladesh

[2] Department of Statistics, Jahangirnagar University, Savar 1342, Dhaka, Bangladesh

[3] Department of Microbiology and Molecular Genetics, University of Vermont, Stafford Hall, Burlington, VT 05405, USA

[4] Department of Mathematics, Rajshahi University of Engineering & Technology, Rajshahi, Bangladesh

[5] Department of Zoology, University of Rajshahi, Rajshahi, Bangladesh

[6] Universidad Europea del Atlántico, Isabel Torres 21, 39011 Santander, Spain

[7] Universidad Internacional Iberoamericana, 24560 Campeche, Mexico

[8] Universidad Internacional Iberoamericana, Arecibo, Puerto Rico 00613, USA

[9] Universidad de La Romana, La Romana, República Dominicana

[10] University of Valladolid, Valladolid, Spain

Published online: 27 January 2026

Introduction

Human metapneumovirus (hMPV) is a common viral pathogen of acute respiratory tract infection (ARI) contributing to a large number of illnesses worldwide (Williams BG 2022; Hoogen et al. 2001). Although the prevalence of hMPV varies globally from 5 to 15% among children, the altered genotypes can cause higher incidence and larger outbreaks (Williams BG 2022; Hoogen et al. 2001; Haas LE 2013; Hoogen 2004). The virus was first identified in the Netherlands using molecular analysis of nasopharyngeal aspirates from children. These children with hMPV infection developed symptoms, including mild to severe respiratory tract problems, bronchiolitis, cough, and pneumonia (Hoogen et al. 2001).

Human metapneumovirus (hMPV) is one of the most frequent pathogens of respiratory tract infections, disproportionately affects vulnerable populations, including young children, the elderly, and immunocompromised individuals (Haas LE 2013; Hoogen 2004; Hoogen 2003; Kahn JS 2006; Hoogen 2002). Transmission of hMPV occurs via the respiratory secretions from the infected person to the susceptible. Direct exposure to the droplets with the virus and contact with contaminated objects and surfaces can contribute to the rapid spread of the disease (Kahn JS 2006; Hoogen 2002) Severe infection and life-threatening conditions can occur among children and adults with comorbidity, including asthma, chronic lung disease, congenital heart disease, neuromuscular disorders, cancer, and chronic obstructive pulmonary disease (COPD) (Hoogen 2002).

The genetic make-up and virological aspects are important players in pathogenesis and transmission of hMPV. HMPV has a 13.3 kb negative-sense RNA genome containing eight genes: 3'-N-P-M-F-M2-SH-G-L-5'. The F, SH, and G proteins constitute surface glycoproteins (Masante et al. 2014; Bermingham 1999). The matrix protein M is encoded by M and M2 genes and the overlapping ORFs encode for M2-1 and M2-2 proteins (Leyrat 2014; Hoogen 2004). The negative-sense, single-stranded RNA genome encodes eight genes, namely N, nucleocapsid; P, phosphoprotein; M, matrix; F, fusion; M2; SH, small hydrophobic; G, glycoprotein; and L, polymerase (Buchholz 2005; Buchholz 2006). The fusion (F) protein of hMPV is highly conserved among hMPV subgroups, and it shares similar structural topology and approximately 30% amino acid sequence homology with the respiratory syncytial virus (RSV) F protein. The prefusion conformation of hMPV F is meta-stable and undergoes conformational rearrangement to the post-fusion state during the process of membrane fusion (White 2008; Skiadopoulos 2006). As the only target of neutralizing antibodies, hMPV F has been stabilized in both prefusion and post-fusion conformations to facilitate recombinant expression and vaccine development (Battles 2017; Mas V et al. 2016). The nucleoprotein N encapsidates the viral genome in a sheath of oligomerized copies of the protein. These proteins contribute to forming the ribonucleoprotein compound called nucleocapsid (Gonnin 2023; Pan et al. 2020). Targeting multiple essential proteins can be an effective way to inhibit the multiplication of the virus.

Recently, the increased incidence of hMPV across many countries in Asia has been an alarming health issue. However, like many other viruses, specific antivirals and vaccines are not available against hMPV. Focusing on the existing gaps in the availability of hMPV antivirals, we performed this study to find the most suitable initial antiviral candidates and analyze their binding properties and drug potentials against the targeted virus well well-described proteins.

Methods

Preparation, identification and modeling of the proteins

Both protein models were identified based on their resolution (Mandal 2024; Laskowski 1993). These proteins were retrieved from the Research Collaboratory for Structural Bioinformatics Protein Data Bank (PDB). The PDB IDs of the selected proteins were 7SEJ (2.51 Å resolution) and 8PDO (3.10 Å resolution). The binding sites of these retrieved proteins were poorly characterized in the database. As a result, we conducted the docking analysis to predict the best pocket and binding sites. For this purpose, all redundant heteroatoms, ions, and water molecules were removed, and RNA was also removed from the nucleoprotein (hMPV-N), and the missing hydrogen atoms and Gasteiger charges were provided to the protein structures (Colovos 1993; Wiederstein 2007; Narkhede 2020; Agu et al. 2023; Gangwar 2024; Pettersen 2004; Kuriata 2018). We also optimized the hMPV protein's 3-D structures by removing the ions, water molecules, and heteroatoms. We also provided the missing hydrogen atoms and charges to the structures. We use the BIOVA Discovery Studio 2024 Client 24.1 and Swiss-PDB-Viewer for the preparation of the 3-D structures (Laskowski 1993; Colovos 1993; Wiederstein 2007; Narkhede 2020). The predicted models of the target proteins were validated by using the Ramachandran plot analysis in the ProCheck (Laskowski 1993). Further, we estimated the overall quality by using the ERRAT2 program (Colovos 1993). The ProSA webserver (https://prosa.services.came.sbg.ac.at/prosa.php), was used to create an energy plot for the model validation and calculate the Z-score of the selected proteins (Wiederstein 2007). We created the PDB file format of the

selected proteins and their receptor targets for molecular docking.

Ligand preparation

The ligand was built by using the derivatives of plant lead agents against common respiratory diseases. The ligands that are docked with the human metapneumovirus (hMPV) proteins. The 3-D crystal structures of these four compounds, apigenin, 4-terpineol, cinnamaldehyde and xanthoangelol E in SDF format and simplified molecular input line entry system strings were taken from PubChem database (https://pubchem.ncbi.nlm.nih.gov/) for use in the molecular docki ng analysis and pharmacokinetics studies. The ligands were converted to the energetically most stable structure using energy minimization for the following docking (Narkhede 2020; Agu et al. 2023; Gangwar 2024; Pettersen 2004; Kuriata 2018; Nag 2022; Lopez-Blanco 2014). We used two currently available antiviral ribavirin (RBVN) and favipiravir (FPVR) (https://pubchem.ncbi.nlm.nih.gov/compound/Ribavirin) and a drug used against diabetic neuropathy (Cohen 2015) as the control for the molecular docking analysis and pharmacokinetics study.

Molecular docking and protein-ligand interaction analysis

Molecular docking, which is an essential tool for in silico drug discovery, predicts the favored pose of a ligand within the target (receptor) protein by forming a stable (protein-ligand) complex through intermolecular interactions (Colovos 1993). All of the molecular and protein-ligand docking experiments were performed by using the PyRx software (Virtual Screening software, available at https://pyrx.sourceforge.io/) because it offers more accuracy in predicting ligand-protein interactions and is very suitable for multiple ligand docking. We performed docking for all the selected hMPV proteins. We performed blind docking of the selected proteins, and protein grid boxes were prepared accordingly, with respective centers (x, y, z) 230.66, 162.88, 213.49.11 Å (for hMPV-N protein), 10.69, 3.80.93, 53.19 Å (for hMPV-F protein) (Agu et al. 2023; Gangwar 2024; Pettersen 2004). The final visualization of the docked structure was performed using the BIOVA Discovery Studio Visualizer 2024 Client 24.1 (https://discover.3ds.com/discovery-studio-visualizer-download).

Molecular dynamics simulations

We used the representative both protein model for the molecular dynamic simulations (MDS) by CABS-flex 2.0 webserver (http://biocomp.chem.uw.edu.pl/CABSflex2) [29]. In this analysis, we determined the root mean square fluctuation (RMSF) values by simulating the flexibility of protein and proper amino acid interactions and complexes. The system was completed with the simulation time of 10 ns, applying default parameters in respect to the MD trajectory, or the NMR ensemble, for recording the RMSF values (as the measure of protein flexibility) of all individual amino acids residues of hMPV-F, and hMPV-F_apigenin, and hMPV-N, and hMPV-N_apigenin docked complexes (Kuriata 2018; Nag 2022; Lopez-Blanco 2014; Arumugam 2021). Thus, all these analyses find out the conformational stability of protein and protein-ligand complex.

Protein contacts atlas

The Protein Contacts Atlas (PCA) is a platform to visualize and analyze the structural insights and the non-covalent contacts within a single protein, protein complex, and between protein and ligands. We have used the Protein Contacts Atlas (at: https://pca.mbgroup.bio/), to analyze the human metapneumovirus (hMPV-F) fusion protein. We took several outcomes from the analysis, including (a) Chord plots revealing the non-covalent contacts at the atomic level of proteins' secondary structures, (b) Asteroid plot showing the amino acid residues, and (c) Scatter plot matrix providing per-residue statistics (Kayikci 2018; Bader 1985; Kumar 2016).

Non-covalent interaction analysis

We found apigenin and xanthoangelol E as the most potent drug candidates by molecular docking studies against hMPV proteins. Additionally, we selected the hMPV-F_apigenin, hMPV-N_apigenin, HMPV-F_xanthoangelol E, and hMPV-N_xanthoangelol E docked complexes for the non-covalent interaction (NCI) study. The reference RBVN was used for comparison. Atom-atom NCIs analysis in the molecules (hMPV-F_apigenin, hMPV-N_apigenin, hMPV-F_xanthoangelol E and hMPV-N_xanthoangelol E complexes) was conducted depending on the reduced density gradient to determine the non-covalent interactions using Bader's Quantum Theory of Atoms in Molecules (QTAIM). The electron density (ED) was defined by following the previous studies (Kayikci 2018; Bader 1985; Kumar 2016; Bohórquez 2011; Johnson 2010). We evaluated the NCIs using the pro-molecular density of atoms following the equation of previous studies. We used the Multiwfn (http://sobereva.com/multiwfn) package for calculating and visualizing the NCIs (Lu and Chen 2012).

Drug likeness, pharmacokinetics, and ADME-Tox analysis

We perform the ADMET (absorption, distribution, metabolism, excretion, toxicity) analysis for the ligands and the control compound using the SwissADME (http://www.swissadme.ch/), and ADMETlab 2.0 (https://admetmesh.scbdd.com/) (Xiong 2021; Daina 2017). We conducted this analysis to evaluate the (i) ADME-Tox (absorption, distribution, metabolism, excretion, and toxicity), ii) drug-likeness of the ligands by adopting Pfizer Rule, GSK Rule, Golden Triangle criteria, along with the Lipinski's RO5, iii) compounds' bioavailability score by radar plot analysis, (iv) medicinal chemistry properties.

Further, we determined the quantitative structure-activity relationship (QSAR) by using the STopTox server (https://stoptox.mml.unc.edu/). For this analysis, six organs were selected as toxicity points, including acute oral toxicity, acute inhalation toxicity, acute dermal toxicity, skin sensitization, eye irritation and corrosion, and skin irritation and corrosion. Additionally, for toxicity analysis, the compounds were subjected to carcinogenicity prediction via the CarcinoPred-EL web server (http://112.126.70.33/toxicity/CarcinoPred-EL/index.html) (Borba 2022; Zhang 2017).

Results

Model quality assessment and validation of target protein structures

Structural models of the N-RNA complex and fusion proteins of human metapneumovirus (hMPV) were evaluated and validated using ProSA web-based servers. To verify the accuracy of these protein models, the SAVES v6.0 webserver (https://saves.mbi.ucla.edu/) was employed, whereas the ProSA web tool (https://prosa.services.came.sbg.ac.at/prosa.php) was used to assess the quality of the 3-D protein structures. The ProSA results, including the Z-scores and energy plots, are presented in the supplementary file. The ERRAT2 web-based program calculated the overall quality factors for the N-RNA complex and hMPV-F proteins to be 92.97 and 97.79, respectively (Supplementary Fig. 1). The Z-scores for the N-RNA complex and hMPV-F proteins were −9.09 and −7.86, respectively, with energy plots showing sequence positions in favorable regions (Supplementary Fig. 1). Overall, the examined models demonstrated high quality and stability, making these proteins suitable targets for antiviral development. The quality of these protein model structures was further confirmed through Ramachandran Plot analysis using the ProCheck web tool from the EMBL-EBI web server (https://www.ebi.ac.uk/thornton-srv/software/PROCHECK/). According to the ProCheck-mediated Ramachandran plots, approximately 92.6% and 90.4% of the residues were located in the most favored regions of the N-RNA complex and hMPV-F proteins, respectively (Supplementary Fig. 2).

Visualization of docking

The experimental findings demonstrated potent interactions between the four prospective drug candidates of plant-derived natural products as lead agents against common respiratory diseases, along with two standard drugs (FPVR, RBVN) (Table 1), against two human metapneumovirus proteins: nucleoprotein (hMPV-N) (we docked all of the compounds only in the nucleoprotein) and hMPV-F protein. Following the successful docking of these compounds to the proteins, various drug-protein interaction modes were generated, each associated with a specific docking score (binding energy). For both the compounds and docking, the binding mode with the lowest binding energy was considered optimal. The investigation also documented the specific amino acids involved in the drug-protein interactions. Visualization of all docked structures was conducted utilizing BIOVIA Discovery Studio 2024 Client 24.1(https://discover.3ds.com/discovery-studio-visualizer-download). The plant-derived four natural compounds interacting with the proteins with involved amino acid residues and bond types, are explained for all the protein-ligand complexes (Fig. 1).

In this study, apigenin demonstrated the highest affinity for the target proteins hMPV-N and hMPV-F, with binding energies of − 7.6 and −8.0 kcal/mol, respectively (Fig. 2 part A and Fig. 3 part A). This compound formed four hydrophobic interactions with the hMPV-F protein (Fig. 4 part C) and established one conventional hydrogen bond with the LYS283 residue, along with three hydrophobic interactions with the hMPV-N protein (Fig. 5 part C). The hMPV-N protein also interacted with 4-Terpineol, showing a binding affinity of − 5.7 kcal/mol (Fig. 3 part D). The binding of this compound in the specific pocket of the hMPV-N protein was confirmed by two hydrogen bonds between the oxygen of a hydroxyl group on the A chain and the residues PRO215 and GLY255, along with some hydrophobic interactions (Fig. 6 part A). Cinnamaldehyde displayed a strong binding affinity with the hMPV-N protein, with an interaction energy of − 5.3 kcal/mol (Fig. 3 part B). Noteworthy conventional hydrogen bonding was observed between the carbonyl group of the ligand and the ARG293 residue of the A chain (Figure. 5 part B). Xanthoangelol E also formed one conventional hydrogen bond with the LYS283 residue of the A chain in the hMPV-N protein complex, with a binding energy of − 5.1 kcal/mol (Fig. 3 part C and Fig. 4 part D).

Table 1 Drugs (ligands) used for docking with the target protein

Drugs name (PubChem ID)	Structure	Binding energy (kj/mol)		No. of hydrogen bonds		Hydrogen bond interactions		Hydrophobic interactions	
		hMPV-F	hMPV-N	hMPV-F	hMPV-N	hMPV-F	hMPV-N	hMPV-F	hMPV-N
4-Terpineol (CID11230)	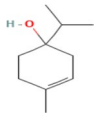	− 5.8	− 5.7	1	2	GLY A:225	PRP A:215, GLY A:255	VAL A:118, PHE A:256	ALA A:113, ALA A:117, PHE A:256
Cinnamaldehyde (CID637511)	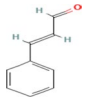	− 5.4	− 5.3	1	1	TYR A:310	ARG A:293	LEU A:105, GLU A:305, ASP A:306, TYR A:319, LYS A:362	GLY A:262, VAL A:263, ARG A:266, VAL A:285, THR A:286, TYR A:289
Apigenin (CID5280443)	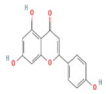	− 8.00	− 7.6	0	1	No hydrogen bonds	LYS A: 283	TRP B:43, THR F:114, ALA F:117, LYS F:254, PHE F:256, ASP F:325, ASP F:336	VAL B:263, ILE B:264, ALA A:280, LEU A:8, SER A:9
Xanthoangelol E (CID10022050)	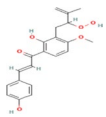	− 6.7	− 7.6	0	1	No hydrogen bonds	LYS A:283	ARG B:91, ALA F:117, PRO F:215, LYS F:254,	VAL B:263, ILE B:264, LEU B:332, LEU A:8, SER A:9, ALA A:280, GLU A:287
Favipiravir (CID492405)	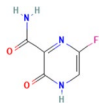	− 6.7	− 6.5	7	3	TYR C:23, GLU C:25, SER A:291, CYS A:292, TYR A:385, SER A:443, CYS A:407	ASP A:28, GLN A:216, VAL A:218,	PRO A:441	SER A:88
Ribavirin (CID37542)	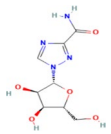	− 6.3	− 5.1	4	4	THR A:114, PRO A:215, ARG A:253, GLY A:255	SER A:9, ASP A:10, GLU A:287, ASN A:317	ALA A:117	GLU A:281, LYS A:283
Gabapentin (CID3446)	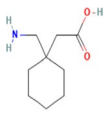	− 5.2	− 5.2	2	2	PRO F:215, ARG F:253	LEU A:8, LYS A:283	ALA F:117, PHE F:256	ASP A:10, VAL B:263

Docking studies of the hMPV-F protein showed excellent interactions with these ligands (Fig. 1). 4-terpineol formed one conventional hydrogen bond with the GLY255 residue of the A chain and two hydrophobic interactions, with a binding energy of -5.7 kcal/mol (Fig. 2 part D and Fig. 3 part A). Cinnamaldehyde and xanthoangelol E interacted with the hMPV-F protein, showing binding affinities of -5.3 and − 7.6 kcal/mol, respectively (Fig. 2 part B-C). Cinnamaldehyde formed one conventional hydrogen bond with the TYR310 residue of the A chain, and both cinnamaldehyde and xanthoangelol E also engaged in some hydrophobic interactions (Fig. 3 part B and D).

In this study, we also predicted the binding potential of two standard antivirals and gabapentin as control drug targeting both the hMPV-N and hMPV-F proteins. FPVR exhibited binding energies of − 6.5 and − 6.7 kcal/mol, while RBVN showed values of − 5.1 and − 6.3 kcal/mol (Fig. 3 part E–F and Fig. 2 part E–F). When interacting with the hMPV target proteins, FPVR and RBVN displayed hydrogen bonds and hydrophobic interactions. RBVN and FPVR formed four and three conventional hydrogen bonds with the hMPV-N protein, respectively. The hMPV-F protein also interacted with RBVN and FPVR, forming four and seven conventional hydrogen bonds, respectively (Fig. 5 part E–F and Figure part 4 E–F). Gabapentin also interacted with two

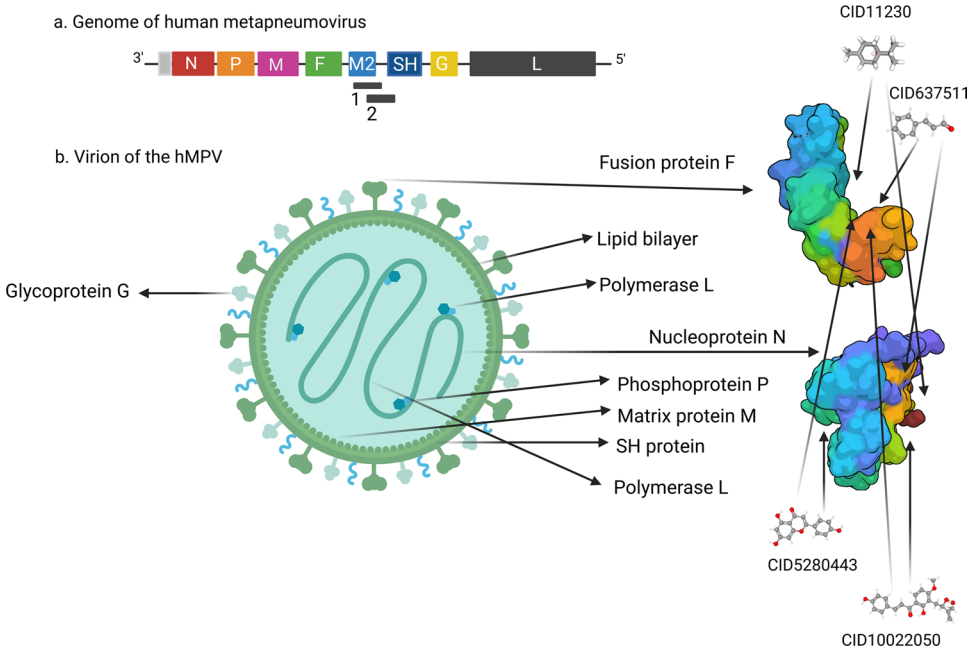

Fig. 1 Human metapneumovirus **a** major genes encoding necessary proteins and other macromolecules, and **b** virion with the target proteins and ligands for antivirals

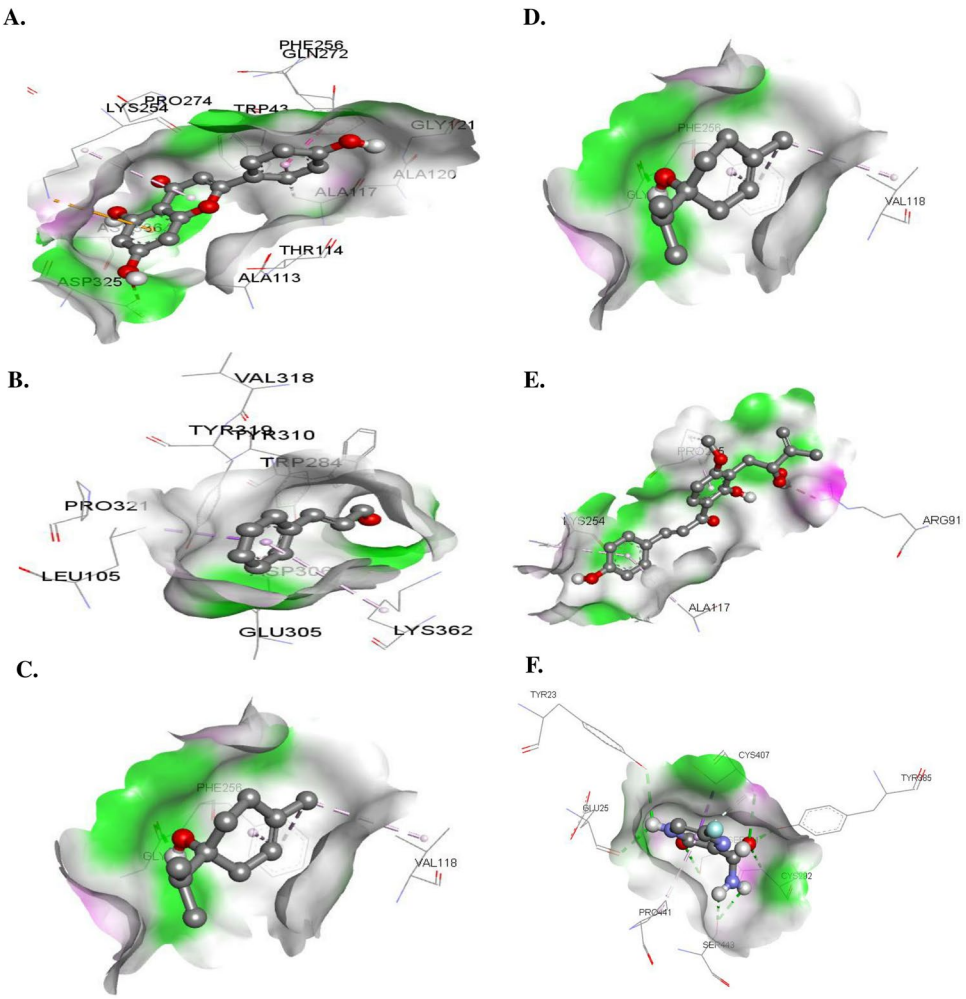

Fig. 2 The 3-D elucidation of molecular docking between hMPV-F protein and four plant-derived respective ligands against common respiratory disease and two standard (FPVR and RBVN): **A** hMPV-F_apigenin, **B** hMPV-F_cinnamaldehyde, **C** hMPV-F_xanthoangelol E, **D** hMPV-F_4-terpineol, **E** hMPV-F_RBVN and **F** hMPV-F_FPVR. hMPV-F: Human metapneumovirus fusion protein, FPVR: favipiravir, RBVN: ribavirin

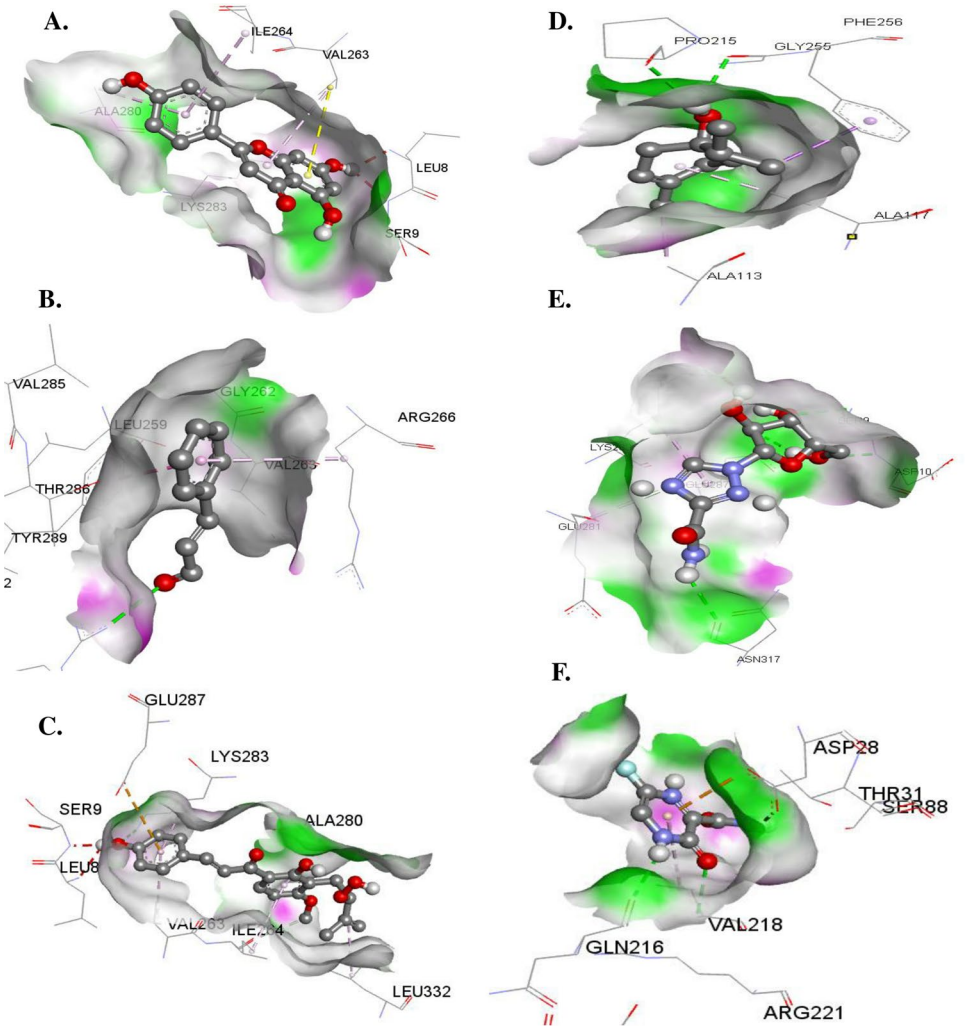

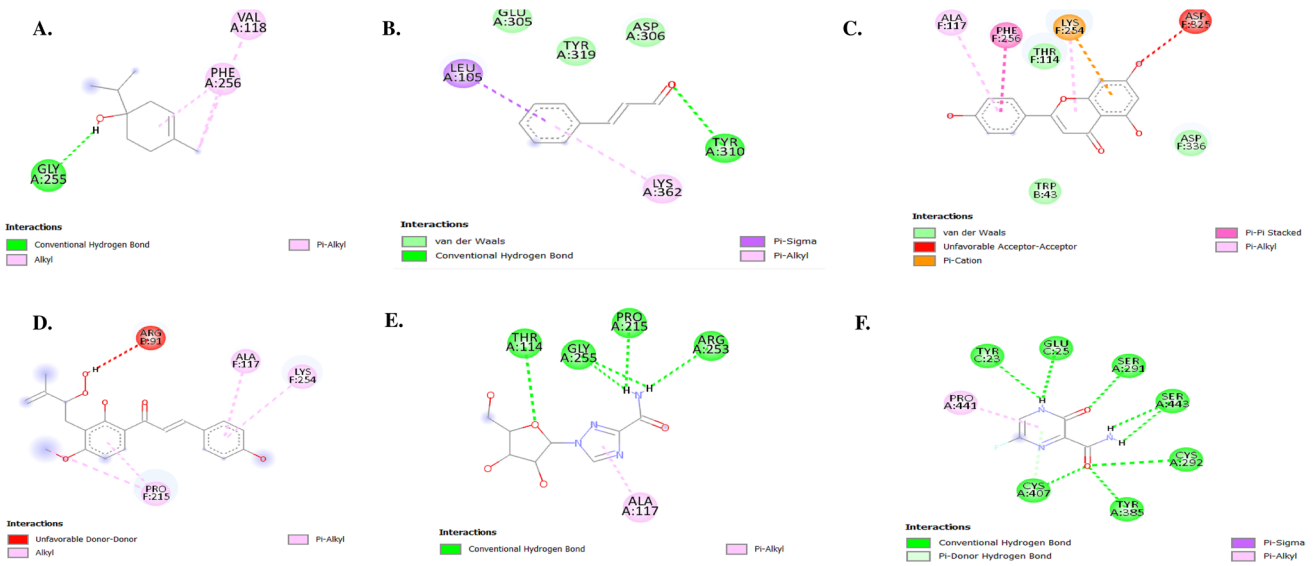

Fig. 3 The 3-D elucidation of molecular docking between hMPV-N protein and four plant-derived respective ligands against common respiratory disease and two standard (FPVR and RBVN): **A** hMPV-N_apigenin, **B** hMPV-N_cinnamaldehyde, **C** hMPV-N_xanthoangelol E, **D** hMPV-N_4-terpineol, **E** hMPV-N_RBVN and **F** hMPV-N_FPVR. hMPV-N: Human metapneumovirus nucleoprotein, FPVR: favipiravir, RBVN: ribavirin

Fig. 4 Two-dimensional (2-D) elucidation of interaction between hMPV-F (human metapneumovirus fusion protein) and ligands: **A** 4-terpineol, **B** cinnamaldehyde, **C** apigenin, **D** xanthoangelol E, **E** ribavirin, **F** favipiravir. The number of conventional hydrogen bonds is one in hMPV-F_4-terpineol and hMPV-F_cinnamaldehyde, and four and seven in hMPV-F_ribavirin and hMPV-F_favipiravir complexes. Apigenin and xanthoangelol E displayed no conventional hydrogen bond against hMPV-F

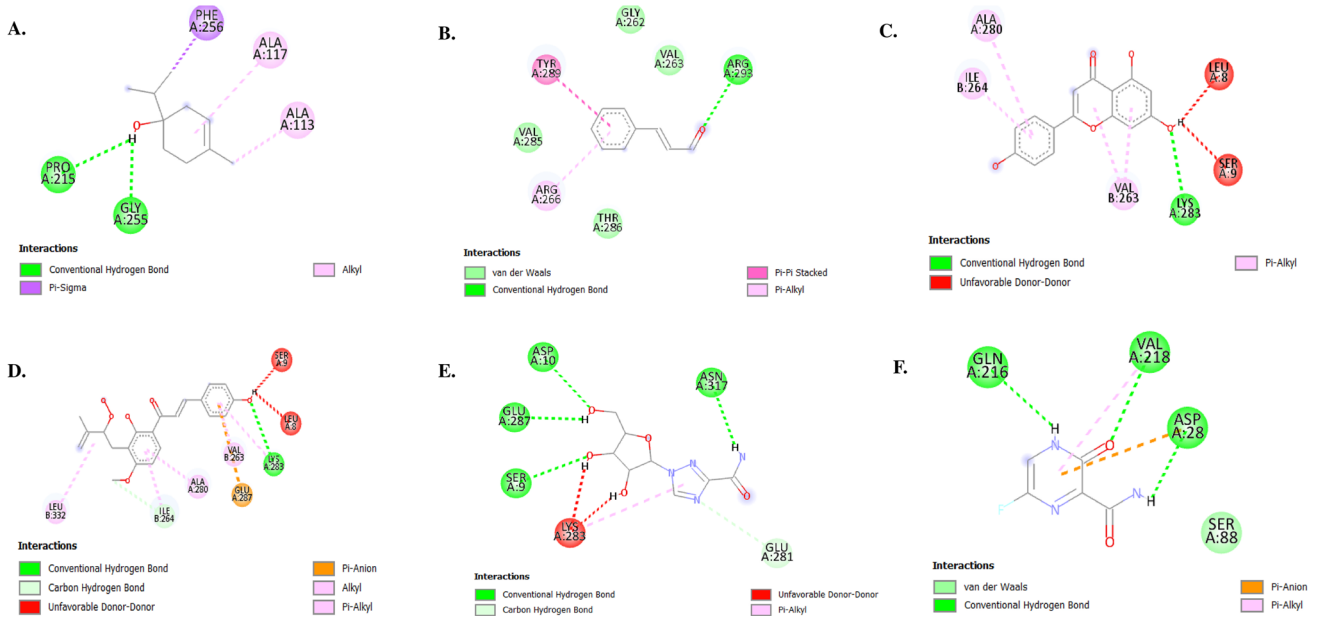

Fig. 5 Two-dimensional (2-D) elucidation of interaction between hMPV-N (human metapneumovirus nucleoprotein) and ligands: **A** 4-terpineol, **B** cinnamaldehyde, **C** apigenin, **D** xanthoangelol E, **E** ribavirin, **F** favipiravir. The number of conventional hydrogen bond is one in hMPV-N_apigenin, hMPV-N_cinnamaldehyde and hMPV-N_xanthoangelol E, four in hMPV-N_ribavirin and hMPV-N_favipiravir complexes. Compound 4-terpineol displayed two conventional hydrogen bonds against hMPV-N

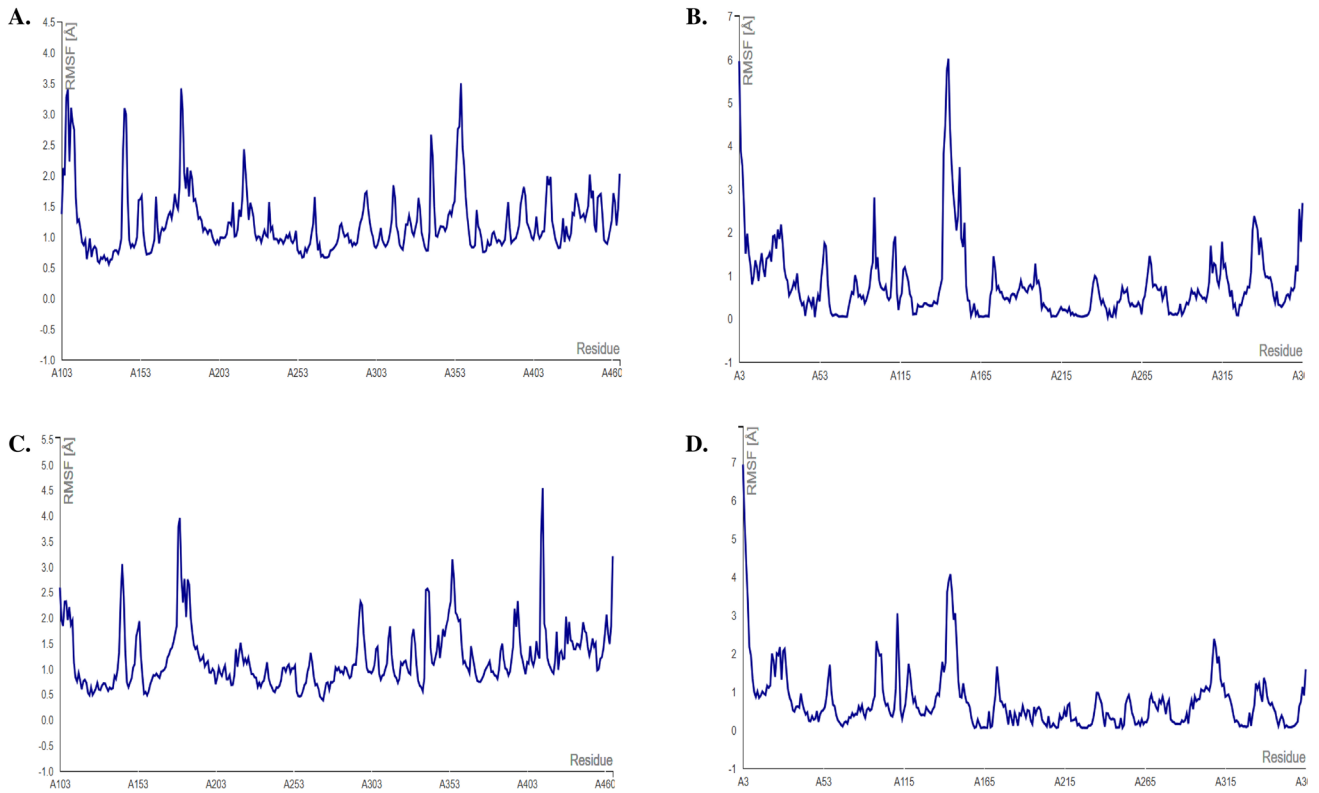

Fig. 6 The CABS-flex-based MDS analysis showed RMSF (root mean square fluctuation) plot to authenticate the protein structural stability for unbound **A** hMPV-F, **B** hMPV-F_apigenin, and **C** hMPV-N **D** hMPV-N_apigenin docked complexes. hMPV-F: Human metapneumovirus fusion protein, hMPV-N: Human metapneumovirus nucleoprotein

hydrogen bonds and showed −5.2 kcal/mol binding affinity with both proteins depicted in Table 1 and Supplementary Fig. 3.

Molecular simulations

We conducted molecular dynamic simulation using CABS-flex 2.0 to compute the RMSF values hMPV-F, and hMPV-F_apigenin, hMPV-N, and hMPV-N_apigenin docked complexes (Fig. 5 part A–D). We found low fluctuation and higher stability in the receptor protein conformation after molecular docking. This study demonstrated that both proteins have multiple amino acids in different regions to form a significantly stable complex with the ligand. In our study, hMPV-F protein displayed amino acid residues with RMSF values within 0.00 and 3.00 Å, while a total of 847, 680, and 688 amino acid residues of the docked complexes hMPV-F_apigenin, hMPV-N, and hMPV-N_apigenin, respectively, displayed the RMSFs within the mentioned range. On the other hand, hMPV-F, hMPV-F_apigenin, hMPV-N

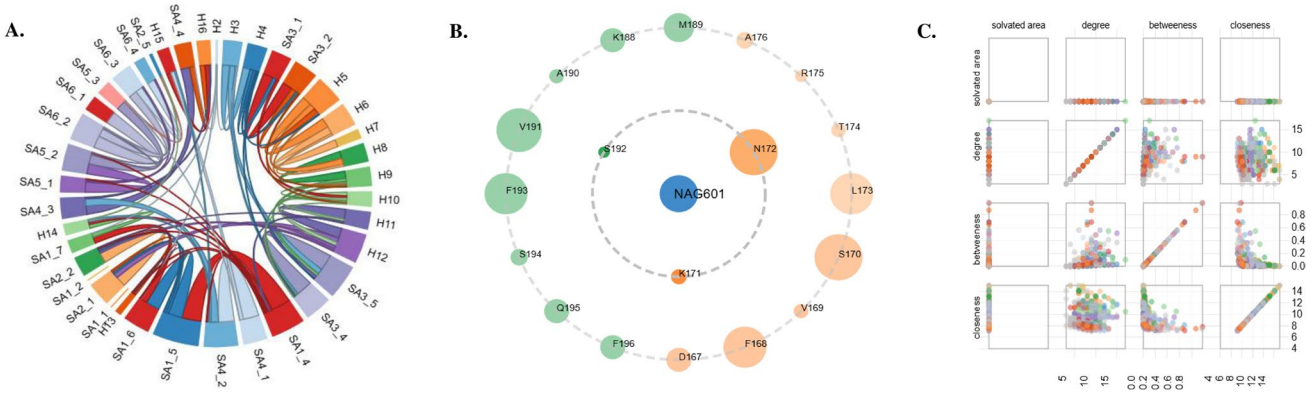

Fig. 7 Protein contact atlas of selected proteins of hMPV—F protein. **A** a Chord plot showing the secondary structure elements of the protein necessary in shaping the tertiary structure, **B** an Asteroid plot with the most active residue for ligand-protein interaction through conventional hydrogen bonds (the number of node sizes depicts the number of contacts), and **C** provides a Scatter plot of the residues. hMPV-F: Human metapneumovirus fusion protein

Table 2 The highly flexible amino acid residues recorded for hMPV-F, hMPV-F_apigenin, hMPV-n and hMPV-N_apigenin complexes with RMSF values > 3 Å

hMPV-F		hMPV-F_apigenin		hMPV-N		hMPV-N_apigenin	
Residues	RMSF (Å)	Residues	RMSF (Å)	Residues	RMSF (Å)	Residues	RMSF (Å)
GLY63	3.602	GLY63	3.211	SER99	3.324	ASN362	3.882
PRO64	3.652	LYS143	3.059	VAL342	3.417	LYS363	5.674
GLY106	3.276	LYS179	3.789	PRO343	3.745	ILE364	7.564
ALA107	3.407	ASN180	3.961	ASN344	3.953	ASN365	8.96
ALA109	3.109	ASN412	3.617	THR345	3.177	LEU3	6.951
LYS179	3.423	GLN413	4.544	GLU346	3.224	GLN4	4.495
ASN180	3.072	GLN346	3.28	PHE348	3.616	GLY5	4.406
THR357	3.505	GLU349	3.014	SER349	3.647	ILE6	3.41
PHE103	4.935	ASN353	3.575	ASN362	4.68	SER99	3.06
LYS143	3.731	ILE354	5.025	LYS363	6.758	SER142	3.615
THR144	3.201	SER355	4.355	ILE364	8.513	SER143	3.917
LYS295	3.99	THR356	4.334	ASN365	10.142	GLY144	4.08
LYS296	5.165	THR357	3.642	LEU3	5.969	ASN145	3.63
GLY297	7.243	ASN358	3.639	GLN4	3.886	–	–
TYR299	4.007	PRO452	5.061	GLY5	3.534	–	–
SER355	3.047	GLN453	3.776	SER142	3.831	–	–
THR356	3.068	–	–	SER143	4.472	–	–
PRO452	5.88	–	–	GLY144	5.746	–	–
GLN453	4.331	–	–	ASN145	6.022	–	–
ASP454	3.577	–	–	ILE146	4.407	–	–
–	–	–	–	PRO147	3.568	–	–
–	–	–	–	PRO152	3.513	–	–

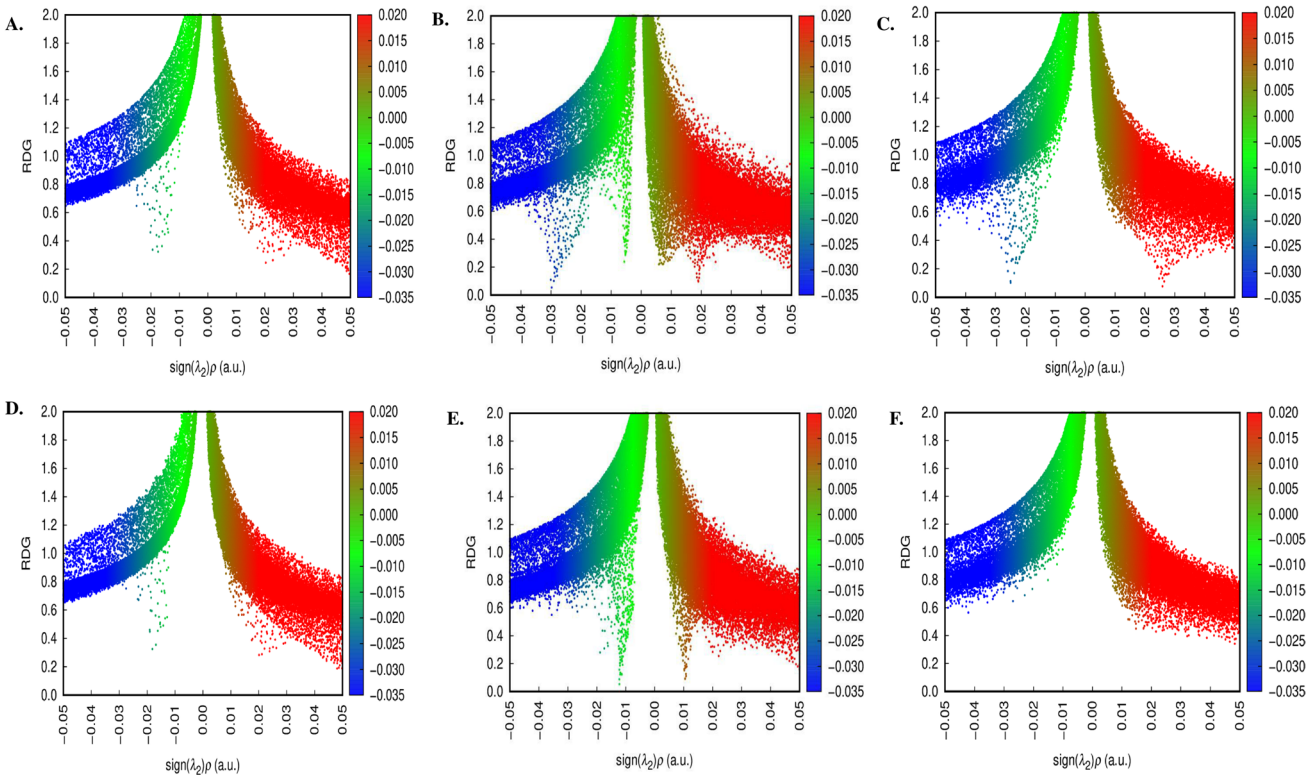

Fig. 8 Non-covalent interaction (NCI) analysis for **A** hMPV-N_apigenin, **B** hMPV-N_xanthoangelol E, **C** hMPV-N_RBVN, **D** hMPV-F_apigenin, **E** hMPV-F_xanthoangelol E, and **F** hMPV-F_RBVN docked complexes based on the reduced density gradient (RDG) using Multiwfn. In the scatter plots, red color indicates the steric effect (repulsion) in regions with sign(λ 2) ρ >0, green color represents VDW (van der Waals) interactions in regions with sign (λ 2 with sign(λ 2) ρ) ρ = 0, blue color in the regions < 0 displays hydrogen bonding

and hMPV-N_apigenin complexes had average RMSFs of 1.276, 1.309, 0.837 and 0.776 Å, respectively. The hMPV-F, hMPV-F_apigenin, hMPV-N and hMPV-N_apigenin complexes displayed highly flexible residues with RMSFs: 3.047 to 7.243 Å (for 20 residues), 3.014 to 5.061 Å (for 16 residues), 3.177 to 10.142 Å (for 22 residues) and 3.06 to 8.96 Å (for 13 residues) (Table 2).

Protein contacts atlas profiles

We performed a PCA analysis on the hMPV-F protein of human metapneumovirus (Fig. 7). The Chord plots illustrated the essential secondary structure components contributing to the protein's tertiary structure and functionality. These plots indicated a greater number of loops with significant residue contact within the proteins. The Asteroid plots revealed the central residues with the strongest ligand interactions via hydrogen bonds (Fig. 7 part B), with the inner circle (first shell) containing NAG601 residues in the hMPV-F protein's asteroid plots. The Scatter plot (Fig. 7 part C) provided quantitative data per residue, including solvated area, degree, betweenness, and closeness, with all scatter plots predicting higher acceptable values for the study protein.

Non-covalent interaction analysis

Non-covalent interaction analysis was conducted to examine intramolecular and intermolecular bonding structures using the RDG indicator. In this study, hMPV-F_apigenin, hMPV-N_apigenin, hMPV-F_xanthoangelol E, and hMPV-N_xanthoangelol E showed a higher number of spikes in steric interaction regions, indicating sign (λ2)ρ (Fig. 8 part A–D), evident in the π-interactions (Figs. 4 and 5). The hMPV-N_apigenin complex exhibited strong spikes in steric interaction regions (sign(λ2)ρ) (Fig. 8 part A) with three π-interactions (Fig. 5 part C). Similarly, the hMPV-F_apigenin complex showed higher spikes in steric regions (sign(λ2)ρ) with three π-interactions (Figs. 4, 5 and 8D). The hMPV-F_xanthoangelol E and hMPV-N_xanthoangelol E also displayed higher spikes in steric regions (sign(λ2) ρ) with three and four π-interactions, respectively. The six protein-ligand complexes also showed peak points with sign(λ2)ρ by H-bonds, indicating stronger interaction. The non-covalent interaction regions, with sign(λ2)ρ≈0 represented by green color, indicated the VDW bonds (Fig. 8).

Fig. 9 The bioavailability radar of the ligands, evaluated through SwissADME web tool. The plant-derived compounds used were **A** 4-terpineol, **B** cinnamaldehyde, **C** apigenin, **D** xanthoangelol, references, **E** favipiravir, and **F** ribavirin. The colored zone specifies the relevant physicochemical space for oval bioavailability

Bioavailability analysis

The bioavailability of the plant-derived ligands was provided by using the radar plot (Fig. 9). We also provided the bioavailability score of the two reference ligands, including favipiravir and ribavirin. We found that the ligands, 4-terpineol, xanthoangelol E, apigenin, and cinnamaldehyde had acceptable bioavailability scores in the majority of the parameters compared to the reference antivirals (Fig. 9). They showed improved drug-likeness compared to the existing antiviral compounds. The bioavailability score was 0.68 for all the ligands.

Evaluation of acute toxicity and carcinogenicity of the ligands

Evaluation of acute toxicity and carcinogenicity of the ligands was conducted using STopTox (Figs. 10 and 11). We predicted the end-point toxicity for apigenin and

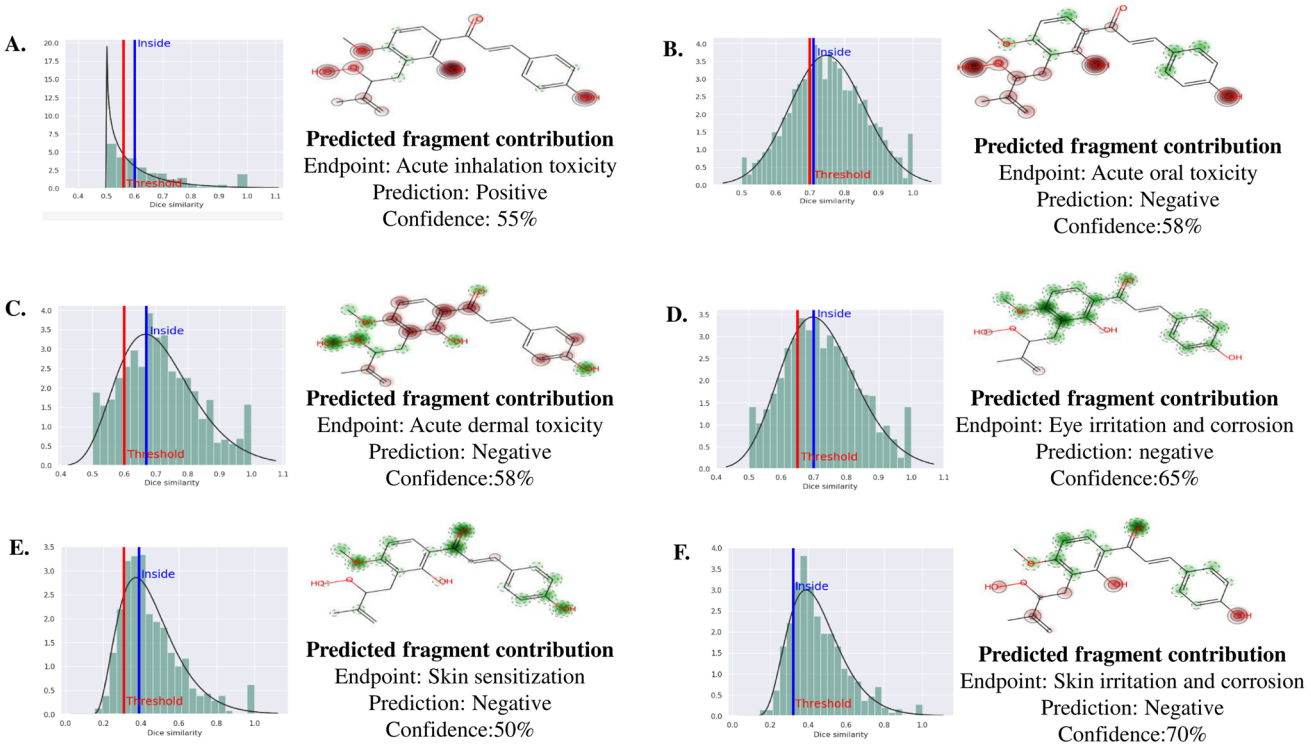

Fig. 10 STopTox-generated six-pack end-points toxicity for xanthoangelol E. **A** Acute Inhalation toxicity, **B** Acute Oral toxicity, **C** Acute Dermal toxicity, **D** Eye Irritation and Corrosion, **E** Skin Sensitization, **F** Skin Irritation and Corrosion. In each model, atoms and structural fragments determining the toxicity are indicated with brown continuous lines, and the regions reducing the toxicity are indicated with green dashed lines

xanthoangelol E. The most active ligands with antiviral properties against hMPV-F and hMPV-N proteins showed highly acceptable values in the fragment contributions (atoms and structural fragments) models. We found a negative prediction for xanthoangelol E ligand in acute dermal toxicity, skin sensitization, eye irritation and corrosion, and skin irritation and corrosion tests with confidence scores of 58, 58, 65, 50, and 70%, respectively (Fig. 10), while acute inhalation toxicity showed a positive confidence score of 55% (Fig. 10). Additionally, apigenin provided acceptable values in three parameters in the STopTox analysis. In three out of six acute toxicity tests, apigenin showed negative predictions with confidence scores ranging from 66–73% (Fig. 11). Additionally, for assessing the carcinogenic potential of all ligands, we utilized the CarcinoPred-EL webserver (http://ccsipb.lnu.edu.cn/toxicity/CarcinoPred-EL/b), which employs three machine learning techniques (Ensemble SVM, Ensemble RF, and Ensemble XGBoost) to estimate carcinogenicity by calculating average probabilities (Table 3). All compounds in our research exhibited probabilities below 0.5, with apigenin showing the lowest values: 0.27, 0.26, and 0.44 in the SVM, RF, and XGBoost models, respectively.

Evaluation of ADMET profiles of the ligands

Assessment of the ADMET profiles of the ligands revealed through SwissADME analysis that 4-terpineol complies with Lipinski's rule of five for drug-likeness, having a molecular weight of 154.25 g/mol (less than 500 g/mol), one H-bond donor (not exceeding 5), one H-bond acceptor (not exceeding 10), one rotatable bond (not exceeding 10), a Topological Polar Surface Area (TPSA) of 20.23 $Å^2$ (< 140 $Å^2$), 11 heavy atoms (not exceeding 36), and an AlogP value not exceeding 5 (Table 4). Similarly, other three ligands adhered to Lipinski's rule of five with no violations, as shown in Table 5. The low logP value and the number of H-bond donors and acceptors of the four ligands suggested good absorption and permeation with balanced hydrophobicity and hydrophilicity. Terpineol and xanthoangelol were found to be BBB positive, and all ligands exhibited high gastrointestinal (GI) absorption. The analysis indicated that 4-terpineol and cinnamaldehyde did not respond to CYP1A2, CYP2C19, CYP2C9, CYP2D6, and CYP3A4 inhibitors. Apigenin responded to CYP1A2, CYP2D6, and CYP3A4 inhibitors, while xanthoangelol E responded to CYP2C9 and CYP3A4 inhibitors. CYP3A4 was identified as a non-substrate/non-inhibitor, suggesting potential liver metabolism. SwissADME analysis showed that apigenin

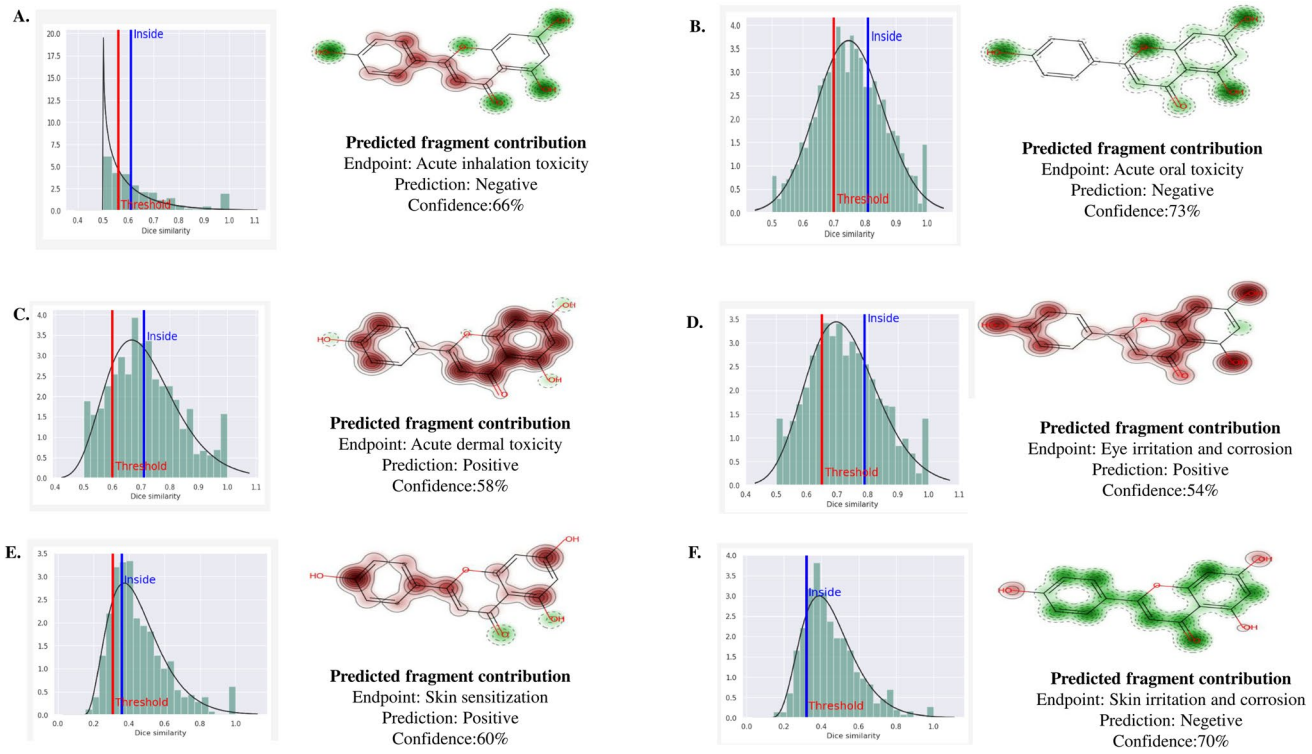

Fig. 11 STopTox-generated six-pack end-points toxicity for apigenin. **A** Acute Inhalation toxicity, **B** Acute Oral toxicity, **C** Acute Dermal toxicity, (D) Eye Irritation and Corrosion, **E** Skin Sensitization, **F** Skin Irritation and Corrosion. In each model, atoms and structural fragments determining the toxicity are indicated with brown continuous lines, and the regions reducing the toxicity are indicated with green dashed lines

Table 3 Carcinogenicity prediction for plant-derived ligands against common respiratory diseases and standard antivirals

Ligand	Method	CDK	CDKExt	CDKGraph	KR	KRC	MACCS	Pubchem	Average	Class
4-terpineol	RF	0.35	0.38	0.16	0.38	0.38	0.34	0.37	0.34	NC
	SVM	0.30	0.30	0.37	0.41	0.43	0.32	0.51	0.38	NC
	XGBOOST	0.07	0.19	0.47	0.45	0.85	0.63	0.76	0.49	NC
Cinnamaldehyde	RF	0.16	0.20	0.28	0.42	0.33	0.23	0.21	0.26	NC
	SVM	0.41	0.38	0.59	0.62	0.54	0.27	0.24	0.44	NC
	XGBOOST	0.07	0.19	0.47	0.45	0.78	0.63	0.76	0.48	NC
Apigennin	RF	0.26	0.27	0.30	0.27	0.19	0.35	0.21	0.27	NC
	SVM	0.18	0.24	0.29	0.35	0.26	0.24	0.25	0.26	NC
	XGBOOST	0.07	0.19	0.47	0.45	0.51	0.63	0.76	0.44	NC
Xanthoangelol E	RF	0.41	0.42	0.54	0.48	0.54	0.31	0.27	0.42	NC
	SVM	0.25	0.41	0.37	0.55	0.44	0.25	0.38	0.38	NC
	XGBOOST	0.07	0.19	0.47	0.45	0.57	0.63	0.76	0.45	NC
Favipiravir	RF	0.41	0.45	0.24	0.51	0.45	0.20	0.35	0.37	NC
	SVM	0.31	0.46	0.17	0.49	0.61	0.27	0.39	0.39	NC
	XGBOOST	0.07	0.19	0.47	0.45	0.84	0.63	0.76	0.49	NC
Ribavirin	RF	0.42	0.45	0.33	0.48	0.27	0.45	0.45	0.41	NC
	SVM	0.28	0.41	0.41	0.33	0.26	0.40	0.42	0.36	NC
	XGBOOST	0.07	0.19	0.47	0.45	0.22	0.63	0.76	0.40	NC

and xanthoangelol E met all drug-like filters, including Ghose (with 4-terpineol having 1 violation and cinnamaldehyde having 2 violations), Veber, Egan, and Muegge, which define drug-likeness constraints through various parameters. A bioavailability score of 0.55 for all four ligands indicated a 55% probability of rat bioavailability. Alerts were observed for PAINS and Brenk, except for apigenin, indicating the specificity of the compounds. All ligands performed well in the ADMET analysis, with some exceptions, and exhibited favorable pharmacokinetic properties (Table 5).

Table 4 Physicochemical properties of ligands

	Ligands			
	4-Terpineol	Apigenin	Cinnamaldehyde	Xanthoangelol E
Physicochemical properties				
Molecular weight	154.25 g/mol	270.24 g/mol	132.16 g/mol	370.40 g/mol
Number of heavy atoms	11	20	10	27
Number of H-bonds donors	1	3	0	3
Number of H-bond acceptors	1	5	1	6
Number of rotatable bonds	1	1	2	8
TPSA	20.23 $Å^2$	90.90 $Å^2$	17.07 $Å^2$	96.22 $Å^2$

Table 5 ADMET properties of the compounds

	Ligands			
	4-Terpineol	Apigenin	Cinnamaldehyde	Xanthoangelol E
Pharmacokinetics				
GI adsorption	High	High	High	High
BBB permeant	Yes	No	Yes	No
CYP1A2 inhibitor	No	Yes	No	No
CYP2C19 inhibitor	No	No	No	No
CYP2C9 inhibitor	No	No	No	Yes
CYP2D6 inhibitor	No	Yes	No	No
CYP3A4 inhibitor	No	Yes	No	Yes
Log K_p (skin permeation)	− 4.93 cm/s	− 5.80 cm/s	− 5.76 cm/s	− 5.41 cm/s
Druglikeness				
Lipinski	Yes; 0 violation	Yes; 0 violation	Yes; 0 violation	Yes; 0 violation
Ghose	No; 1 violation: MW < 160	Yes	No; 2 violations: MW < 160, #atoms < 20	Yes
Veber	Yes	Yes	Yes	Yes
Egan	Yes	Yes	Yes	Yes
Muegge	No; 2 violations: MW < 200, Heteroatoms < 2	Yes	No; 2 violations: MW < 200, Heteroatoms < 2	Yes
Bioavailability Score	0.55	0.55	0.55	0.55
Medical chemistry				
PAINS	0 alert	0 alert	0 alert	0 Alert
Brenk	1 alert: isolated_alkene	0 alert	2 alerts: aldehyde, michael_acceptor_1	3 alerts: isolated_alkene, michael_acceptor_1, peroxide
Leadlikeness	No; 1 violation: MW < 250	Yes	No; 1 violation: MW < 250	No; 3 violations: MW > 350, Rotors > 7, XLOGP3 > 3.5
Synthetic accessibility	3.28	2.96	1.65	3.84

Overall, the results showed that apigenin and xanthoengelol E provide good docking score and binding affinities against hMPV proteins, suitable stability of the protein-ligand complexes and acceptable pharmacokinetic properties than other candidates which make both of them promising primary candidates in this study.

Discussion

Identifying compounds that exhibit a broad antiviral spectrum by targeting highly conserved structures has proven to be effective against a wide array of viruses (Mandal 2024; Hsieh 2022). First, to the best of our knowledge, this study represents the most comprehensive investigation of human metapneumovirus (hMPV) drug discovery using plant derived flavonoids. Our predicted flavonoids demonstrated the strongest binding affinity and the lowest binding energy,

ranging from −5.1 to − 8.00 kcal/mol, when tested against the anticipated stable structures of the hMPV-N protein and the human metapneumovirus (hMPV-F) fusion protein. We compared the docking results of selected compounds with standard compounds and all of the compounds have stronger binding affinity towards both hMPV protein (Swapna 2024; Daipule 2019). Any values below −5.0 kcal/mol during molecular docking between the ligand and target protein are considered significantly stronger bindings (Mandal 2024; Laskowski 1993; Colovos 1993; Wiederstein 2007; Narkhede 2020). In the majority of the protein-ligand interactions, hydrogen bonds, VWB, and non-covalent bonds were detected. In this context, apigenin and xanthoangelol E have the acceptable binding potentials to the predicted protein models. Compared to previous studies, we predicted the lowest binding energy against these proteins (Hsieh 2022; Whitehead 2023; Tawar 2009; Gonnin 2023). Second, we explored a large library of compounds to predict antivirals against metapneumovirus (hMPV), making them as candidate therapeutic molecules that could interact in an acceptable level. When interacting with various proteins, all of the anticipated ligands offer flexibility. Further important information about these compounds' antiviral activity can be added by wet lab study. Third, by using some of the acceptable techniques for predicting stable interactions, we have assessed our target protein models. In the Ramachandran plot assay, SAVES v6.0 webserver analysis, and ProSA analysis, we found that the chosen proteins of the N-RNA complex and human metapneumovirus (hMPV-F) fusion protein had acceptable level of stability. Previous studies have also used these servers and tools to predict the stability of the protein models (Mandal 2024). In comparison to earlier research, the predicted protein models' Z-score and ERRAT overall quality factor were significantly higher than the accepted limit.

The selection of hMPV proteins was based on their significance in virulence and infection. The human metapneumovirus (hMPV-F) fusion protein is essential for viral entry and is a key target of neutralizing antibodies and vaccine development. The hMPV polymerase (L) binds an obligate cofactor, the phosphoprotein (P). During replication and transcription, the L/P complex traverses the viral RNA genome, which is encapsidated within nucleoproteins (N) (Tawar 2009; Gonnin 2023; Bergh 2022). After choosing the suitable proteins, ligands were screened using prior studies as a guideline. Blind docking was used to find the right protein pockets. The two proteins under investigation showed different binding scores, and the docking results' lowest binding energy was used to determine the pockets. We found that apigenin had the best docking score of all the docked proteins, according to the visualization of the docking results, followed by xanthoangelol E. For the model proteins, we contrasted our results with those of remdesivir and favipiravir. However, we found that our selected ligands were more compatible with the lowest binding energy for the target proteins.

Fourth, in the molecular simulation, we also found that both proteins and their docked compound with apigenin had multiple residues with suitable flexibility and deformability scores to provide an acceptable binding. It has been reported that the residue RMSFs of 1.00–3.00 Å maintained protein conformational stability (Mandal 2024; Bhattacharya 2023; Wang 2020). While some other studies have shown RMSF values below 3 Å, we found average RMSF values of 1.27 Å for the amino acid residues of hMPV-F and 0.837 Å for the hMPV-N protein, which is a highly acceptable result. Additionally, the average RMSFs for the hMPV-F_apigenin and hMPV-N_apigenin complexes were 0.837 and 0.776 Å, respectively. This explains the low fluctuation in the receptor protein conformation after molecular docking with apigenin, signifying the protein-ligand complex stability as has been demonstrated earlier (Bhattacharya 2023; Wang 2020). Additionally, both the protein contact atlas and NCI analysis also showed significantly acceptable scores for the predicted docked complexes.

Fifth, in the pharmacokinetics, toxicity, bioavailability, and carcinogenicity analysis, these compounds have provided acceptable values, which can be modified further to reduce the existing toxicity. Compared to earlier research, all of the ligands displayed a good bioavailability score of 0.68. The toxicity test battery comprises six acute toxicity parameters to predict for small-molecule drugs in their early development process, and these include acute inhalation toxicity, acute oral toxicity, acute dermal toxicity, eye irritation and corrosion, skin sensitization and skin irritation and corrosion. In the acute toxicity analysis based on the STopTox (one of the most accepted toxicity evaluation tools of ligands), xanthoangelol E showed positive results in five parameters, except acute inhalation toxicity and apigenin showed three negative results and three positive results in the six parameters, respectively. Considering carcinogenicity as a highly toxic endpoint for bioactive molecules for drug development purposes, all the plant-based molecules were subjected to carcinogenicity testing in order to know whether the compounds are carcinogens or non-carcinogens. CarcinoPred-EL result showed, all of the compounds were carcinogenicity negative. Additionally, the ligands' pharmacokinetic characteristics were roughly comparable according to the ADMET (absorption, distribution, metabolism, excretion, toxicity) study. Every compound complied with Lipinski's rule of five. Similar to this, all compounds, aside from apigenin, have high GI adsorption and BBB permeability. Given that 4-terpineol and cinnamon aldehyde are CYP3A4 non-substrates/non-inhibitors, the medication

may undergo hepatic metabolism. Based on a comparison of the compounds' ADMET analysis and docking data, it can be concluded that selected ligands favored the interactions with the hMPV virulence proteins and might be evaluated further as initial candidates. Flavonoids have been documented as potent antivirals against other viruses in previous studies. Our study is also providing sufficient evidence on the use of flavonoids as primary antiviral candidates against hMPV (Bhattacharya 2023; Wang 2020; Lani et al. 2016). Apigenin and xanthoangelol E provide best docking scores and binding affinity where protein ligand complex of these candidates also showed acceptable stability in MD simulation. Overall pharmacokinetics properties of these ligands showed acceptable result than other candidates. All of these experiments suggest both apigenin and xanthoangelol E as the initial candidates for future studies.

Though we have conducted a comprehensive analysis using majority of the available tools, this study has several limitations. First, we could not run a 50 to 100 ns simulation due to limitation of resources. However, integration of findings from all of the assays contributed to reduce the impact of one single assay. Second, we could not perform any in-vitro or wet lab analysis, which could add more acceptable insights to our findings. Third, we could not use any of the proteins or ligands derived from laboratory sample, rather reference compounds were used, which might have affected the outcomes. However, our study initially identified suitable compounds to conduct future in-vitro studies. The findings can provide baseline data in developing antiviral compounds against hMPV.

Conclusion

Higher binding affinities for two of the human metapneumovirus virulence proteins were demonstrated by the predicted flavonoid compounds. Multiple binding sites for the chosen ligands were present in the stable protein models. These ligands exhibited considerably acceptable pharmacokinetic characteristics, decreased toxicity, and greater acceptable bioavailability profiles to be suitable initial antiviral candidates. By providing the in-silico insights, this study will provide the baseline data to conduct further in-vitro and in-vivo studies to develop antiviral against hMPV.

Supplementary Information The online version contains supplementary material available at https://doi.org/10.1007/s40203-025-00539-7.

Acknowledgements None.

Author contributions All authors contributed to the study conception and design. Material preparation, data collection and analysis were performed by Hasan Huzayfa Rahaman, Afsana Khan, Nadim Sharif and Wasifuddin Ahmed. The first draft of the manuscript was written by Hasan Huzayfa Rahaman, Nadim Sharif Wasifuddin Ahmed, Nazmul Sharif, Rista Majumder, Silvia Aparicio Obregon, Rubén Calderón Iglesias, Isabel De la Torre Díez, and Shuvra Kanti Dey. All authors read and approved the final manuscript.

Funding The authors declare that no funds, grants, or other support were received during the preparation of this manuscript.

Data availability All data supporting the findings of this study are available within the paper and its Supplementary Information.

Declarations

Conflict of interest The authors declare no conflict of interest.

Ethical approval Not Applicable.

Consent to participate Not Applicable.

Clinical trial number Not applicable.

References

Agu PC, Afiukwa CA, Orji OU et al (2023) Molecular Docking as a tool for the discovery of molecular targets of nutraceuticals in diseases management. Sci Rep 13:13398

Arumugam S, Varamballi P (2021) In-silico design of envelope based multi-epitope vaccine candidate against Kyasanur forest disease virus. Sci Rep 11:17118

Bader RF (1985) Atoms in molecules. Acc Chem Res 18:9–15

Battles MB, Más V, Olmedillas E et al (2017) Structure and immunogenicity of pre-fusion-stabilized human metapneumovirus F glycoprotein. Nat Commun 8:1–11

Bermingham A, Collins PL (1999) The M2–2 protein of human respiratory syncytial virus is a regulatory factor involved in the balance between RNA replication and transcription. Proc Natl Acad Sci 96:11259–11264

Bohórquez HJ, Boyd RJ, Matta CF (2011) Molecular model with quantum mechanical bonding information. J Phys Chem A 115:12991–12997

Borba JV, Alves VM, Braga RC et al (2022) STopTox: an insilico alternative to animal testing for acute systemic and topical toxicity. Environ Health Perspect 130:027012

Buchholz UJ, Biacchesi S, Pham QN et al (2005) Deletion of M2 gene open reading frames 1 and 2 of human metapneumovirus: effects on RNA synthesis, attenuation, and immunogenicity. J Virol 79:6588–6597

Buchholz UJ, Nagashima K, Murphy BR, Collins PL (2006) Live vaccines for human metapneumovirus designed by reverse genetics. Expert Rev Vaccines 5:695–706

Cohen K, Shinkazh N, Frank J et al (2015) Pharmacological treatment of diabetic peripheral neuropathy. Pharm Ther 40:372–388

Colovos C, Yeates TO (1993) Verification of protein structures: patterns of nonbonded atomic interactions. Protein Sci 2:1511–1519

Daina A, Michielin O, Zoete V (2017) SwissADME: a free web tool to evaluate pharmacokinetics, drug-likeness and medicinal chemistry friendliness of small molecules. Sci Rep 7:42717

Daipule K, Goud NS, Sethi A et al (2019) Synthesis, molecular docking simulation, and biological evaluation studies of novel amide and ether conjugates of 2,3-diaryl-1,3-thiazolidin-4- ones. J Heterocyclic Chem. 2019;1–17

De A, Bhattacharya S, Debroy B, Bhattacharya A, Pal K (2023) Exploring the Pharmacological aspects of natural phytochemicals against SARS-CoV-2 Nsp14 through an in Silico approach. Silico Pharmacol 11:12

den Hoogen BG, Herfst S, Sprong L et al (2004a) Antigenic and genetic variability of human metapneumoviruses. Emerg Infect Dis 10:658–666

Gangwar A, Tewari G, Pande C et al (2024) Effect of drying conditions on the chemical compositions, molecular Docking interactions and antioxidant activity of hedychium spicatum Buch-Ham. Rhizome essential oil. Sci Rep 14:28568

Gonnin L, Desfosses A, Bacia-Verloop M et al (2023) Structural landscape of the respiratory syncytial virus nucleocapsids. Nat Commun 14:5732

Haas LE, Thijsen SF, Van Elden L, Heemstra KA (2013) Human metapneumovirus in adults. Viruses 5:87–110

Hsieh CL, Rush SA, Palomo C et al (2022) Structure-based design of prefusion-stabilized human metapneumovirus fusion proteins. Nat Commun 13:1299

Johnson ER, Keinan S, Mori-Sánchez P et al (2010) Revealing noncovalent interactions. J Am Chem Soc 132:6498–6506

Kahn JS (2006) Epidemiology of human metapneumovirus. Clin Microbiol Rev 19:546–557

Kayikci M, Venkatakrishnan AJ, Scott-Brown et al (2018) Visualization and analysis of non-covalent contacts using the protein contacts atlas. Nat Struct Mol Biol 25:185–194

Kumar PSV, Raghavendra V, Subramanian V (2016) Bader's theory of atoms in molecules (AIM) and its applications to chemical bonding. J Chem Sci 128:1527–1536

Kuriata A, Gierut AM, Oleniecki T et al (2018) CABS-flex 2.0: a web server for fast simulations of flexibility of protein structures. Nucleic Acids Re 46:W338–343

Lani R, Hassandarvish P, Shu MH et al (2016) Antiviral activity of selected flavonoids against Chikungunya virus. Antivir Res 133:50–61

Laskowski RA, MacArthur MW, Moss DS, Thornton JM (1993) PROCHECK: a program to check the stereochemical quality of protein structures. J Appl Cryst 26:283–291

Leyrat C, Renner M, Harlos K, Huiskonen JT, Grimes JM (2014) Drastic changes in conformational dynamics of the antiterminator M2-1 regulate transcription efficiency in Pneumovirinae. Elife 3:e02674

López-Blanco JR, Aliaga JI, Quintana-Ortí ES, Chacón P (2014) iMODS: internal coordinates normal mode analysis server. Nucleic Acids Res 42:W271–W276

Lu T, Chen F (2012) Multiwfn: A multifunctional wavefunction analyzer. J Comput Chem 33:580–592

Mandal M, Mandal S (2024) Discovery of multitarget-directed small molecule inhibitors from andrographis paniculata for Nipah virus disease therapy: molecular docking, molecular dynamics simulation and ADME-Tox profiling. Chem Phys Impact 8:100493

Más V, Rodriguez L, Olmedillas E et al (2016) Engineering, structure and immunogenicity of the human metapneumovirus F protein in the postfusion conformation. PLoS Pathog 12:e1005859

Masante C, El Najjar F, Chang A et al (2014) The human metapneumovirus small hydrophobic protein has properties consistent with those of a Viroporin and can modulate viral fusogenic activity. J Virol 88:6423–6433

Nag A, Verma P, Paul S, Kundu R (2022) In Silico analysis of the apoptotic and HPV inhibitory roles of some selected phytochemicals detected from the rhizomes of greater cardamom. Appl Biochem Biotechnol 194:4867–4891

Narkhede RR, Cheke RS, Ambhore JP, Shinde SD (2020) The molecular Docking study of potential drug candidates showing anti-COVID-19 activity by exploring of therapeutic targets of SARS-CoV-2. Eurasian J Med Oncol 4:185–195

Pan J, Qian X, Lattmann S et al (2020) Structure of the human metapneumovirus polymerase phosphoprotein complex. Nature 577:275–279

Pettersen EF, Goddard TD, Huang CC et al (2004) UCSF Chimera—a visualization system for exploratory research and analysis. J Comput Chem 25:1605–1612

Skiadopoulos MH, Biacchesi S, Buchholz UJ et al (2006) Individual contributions of the human metapneumovirus F, G, and SH surface glycoproteins to the induction of neutralizing antibodies and protective immunity. Virology 345:492–501

Swapna K, Srujana M, Mamidala E (2024) Identification of steroidal cardenolides from Calotropis procera as novel HIV-1 PR inhibitors: A molecular Docking & molecular dynamics simulation study. Indian J Med Res 160:78–86

Tawar RG, Duquerroy S, Vonrhein C et al (2009) Crystal structure of a nucleocapsid-like nucleoprotein-RNA complex of respiratory syncytial virus. Science 326:1279–1283

Van Den Bergh A, Bailly B, Guillon P, von Itzstein M, Dirr L (2022) Antiviral strategies against human metapneumovirus: targeting the fusion protein. Antivir Res 207:105405

van den Hoogen BG, de Jong JC, Groen J et al (2001) A newly discovered human pneumovirus isolated from young children with respiratory tract disease. Nat Med 2001:719 – 24

Van den Hoogen BG, Bestebroer TM, Osterhaus ADME, Fouchier RAM (2002) Analysis of the genomic sequence of a human metapneumovirus. Virology 295:119–132

Van den Hoogen BG, van Doornum GJ, Fockens JC et al (2003) Prevalence and clinical symptoms of human metapneumovirus infection in hospitalized patients. J Infect Dis 188:1571–1577

Van Den Hoogen BG, Osterhaus DME, Fouchier RA (2004b) Clinical impact and diagnosis of human metapneumovirus infection. Pediatr Infect Dis 23:S25–S32

Wang L, Song J, Liu A et al (2020) Research progress of the antiviral bioactivities of natural flavonoids. Nat Prod Bioprospect 10:271–283

White JM, Delos SE, Brecher M, Schornberg K (2008) Structures and mechanisms of viral membrane fusion proteins: multiple variations on a common theme. Crit Rev Biochem Mol Biol 43:189–219

Whitehead JD, Decool H, Leyrat C et al (2023) Structure of the N-RNA/P interface indicates mode of L/P recruitment to the nucleocapsid of human metapneumovirus. Nat Commun 14:7627

Wiederstein M, Sippl MJ (2007) ProSA-web: interactive web service for the recognition of errors in three-dimensional structures of proteins. Nucleic Acids Res 35:W407–410

Williams BG, Gouws E, Boschi-Pinto C et al (2022) Estimates of world-wide distribution of child deaths from acute respiratory infections. Lancet Infect Dis 2:25–32

Xiong G, Wu Z, Yi J et al (2021) ADMETlab 2.0: an integrated online platform for accurate and comprehensive predictions of ADMET properties. Nucleic Acids Res 49:W5–W14

Zhang L, Ai H, Chen W et al (2017) CarcinoPred-EL: novel models for predicting the carcinogenicity of chemicals using molecular fingerprints and ensemble learning methods. Sci Rep 7:2118